



# Functional analysis of a tyrosinase gene involved in early larval shell biogenesis in *Crassostrea angulata* and its response to ocean acidification



Bingye Yang<sup>a,b,d</sup>, Fei Pu<sup>a,c,d</sup>, Lingling Li<sup>a,c,d</sup>, Weiwei You<sup>c,d</sup>, Caihuan Ke<sup>a,c,d</sup>, Danqing Feng<sup>a,c,d,\*</sup>

<sup>a</sup> State Key Laboratory of Marine Environmental Science, Xiamen University, Xiamen 361102, China

<sup>b</sup> Xiamen Medical College, Xiamen 361008, China

<sup>c</sup> College of Ocean and Earth Science, Xiamen University, Xiamen 361102, China

<sup>d</sup> Fujian Collaborative Innovation Center for Exploitation and Utilization of Marine Biological Resources, Xiamen University, Xiamen 361102, China

## ARTICLE INFO

### Article history:

Received 18 September 2016

Received in revised form 23 December 2016

Accepted 13 January 2017

Available online 17 January 2017

### Keywords:

Oyster

Shell form

*Ca-tyrA1*

RNAi

Ocean acidification

## ABSTRACT

The formation of the primary shell is a vital process in marine bivalves. Ocean acidification largely influences shell formation. It has been reported that enzymes involved in phenol oxidation, such as tyrosinase and phenoloxidases, participate in the formation of the periostracum. In the present study, we cloned a tyrosinase gene from *Crassostrea angulata* named *Ca-tyrA1*, and its potential function in early larval shell biogenesis was investigated. The *Ca-tyrA1* gene has a full-length cDNA of 2430 bp in size, with an open reading frame of 1896 bp in size, which encodes a 631-amino acid protein that includes a 24-amino acid putative signal peptide. Quantitative reverse transcription-polymerase chain reaction (qRT-PCR) analysis revealed that *Ca-tyrA1* transcription mainly occurs at the trochophore stage, and the *Ca-tyrA1* mRNA levels in the 3000 ppm treatment group were significantly upregulated in the early D-veliger larvae. WMISH and electron scanning microscopy analyses showed that the expression of *Ca-tyrA1* occurs at the gastrula stage, thereby sustaining the early D-veliger larvae, and the shape of its signal is saddle-like, similar to that observed under an electron scanning microscope. Furthermore, the RNA interference has shown that the treatment group has a higher deformity rate than that of the control, thereby indicating that *Ca-tyrA1* participates in the biogenesis of the primary shell. In conclusion, and our results indicate that *Ca-tyrA1* plays a vital role in the formation of the larval shell and participates in the response to larval shell damages in *Crassostrea angulata* that were induced by ocean acidification.

© 2017 Elsevier Inc. All rights reserved.

## 1. Introduction

Anthropogenic CO<sub>2</sub> emissions are currently acidifying the world's oceans. Ocean acidification has significantly reduced the pH of seawater in the past century, which in turn has largely impacted marine organisms, particularly calcifying marine invertebrates. Numerous studies on calcifying marine invertebrates have demonstrated that ocean acidification can impact survival, growth, development, and physiology (Talmage and Gobler, 2010; Hofmann et al., 2010; Valerio et al., 2012). Marine calcifiers are particularly vulnerable to ocean acidification because it is more difficult for them to produce calcium carbonate in acidified water (Orr et al., 2005; Fabry et al., 2008). Research on the early development of *Haliotis discus hannai* has shown that ocean acidification results in decreased fertilization and hatching rates, an increase in malformation rate, and a decrease in settlement (Li et al., 2013). Besides, ocean acidification makes it difficult for pteropods to survive because of instability in their biological skeleton, coupled with shell thinning in

some foraminifera (Li et al., 2013). It has been reported that *Amphiura filiformis* adapts to an increase in calcification and metabolic rates during ocean acidification; however, as pH decreases, the function of wrist muscles is impaired (Wood et al., 2008). Similar findings have also been reported in *Hemicentrotus pulcherrimus* and *Echinometra mathaei* (Shirayama and Thornton, 2005). These findings indicate that the effect of ocean acidification is widespread in marine animals, and induces marine calcifiers to utilize less calcium carbonate (Watson et al., 2012).

Several mollusks are recognized as economically significant calcifiers. However, shells are vital for most mollusk species. It is reported that the typical adult shells of mollusks are composed of several layers, including the external cuticle layer (periostracum) covering the outer surface of the mollusk shell and inner layers containing the CaCO<sub>3</sub> polymorph (calcite and aragonite) (Marin and Luquet, 2004). The shell can be primarily discriminated in gastrulation, and the periostracum is the first observable part of the shell. When larvae develop from gastrulae into early trochophores, an initial shell is formed (Mouëza et al., 2006). To distinguish this from the calcified shell that grows later, Huan et al. (2013) defined this shell as the initial non-calcified shell (InCaS). The InCaS is the first shell during molluscan

\* Corresponding author at: College of Ocean and Earth Science, Xiamen University, 361102, Fujian Province, China.

E-mail address: [dqfeng@xmu.edu.cn](mailto:dqfeng@xmu.edu.cn) (D. Feng).

ontogenesis and thus it is very important to understand molecular mechanisms underlying its biogenesis

It has previously been reported that enzymes involved in phenol oxidation such as tyrosinase and phenoloxidases probably participate in the formation of the periostracum (Checa, 2000). Moreover, tyrosinases have been distinguished in molluscan shells (Marin and Luquet, 2004). Thus, it is important to determine whether tyrosinases take part in InCaS biogenesis. Tyrosinase (EC 1.14.18.1) contains two conserved copper-binding domains, which include conserved amino acid residues. It can catalyze the oxidation of both monophenols and o-diphenols into reactive o-quinones (Chang, 2009) and is involved in mammalian melanogenesis, enzymatic browning reactions in damaged fruits, and sclerotization of insect cuticle (Andersen, 2010; Chang, 2009). Tyrosinase cloned from *Pinctada fucata* has also been shown to be involved in periostracum formation (Zhang et al., 2006). In addition, an earlier research study on InCaS biogenesis in *Crassostrea gigas* reported the successful cloning of a kind of tyrosinase (*cgi-tyr1*) that was expressed in the domain of InCaS by whole mount *in situ* hybridization (WISH), thereby suggesting that it was involved in InCaS biogenesis (Huan et al., 2013). On the other hand, considering that there are multiple tyrosinases and the shell structure of larvae and adults differs, it is essential to understand the relationship between tyrosinases and InCaS formation.

Our current understanding of the impact of ocean acidification on the Fujian oyster *Crassostrea angulata* larvae is limited. In laboratory experiments designed to mimic seawater chemistry in oceans, we tested the impact of short-term exposure to elevated pCO<sub>2</sub> (1500 ppm and 3000 ppm, compared to a control, 400 ppm) on *C. angulata*, which is one of the most important economic aquaculture varieties. In the present study, we cloned a tyrosinase (*Ca-tyrA1* of the oyster *Crassostrea angulata*) and determined by quantitative RT-PCR, whole mount *in situ* hybridization (WISH), and RNA interference (RNAi) that it might be involved in the biogenesis of larval InCaS.

## 2. Materials and methods

### 2.1. Animal and samplings

Adult oysters of *C. angulata* were collected from the coast of Xiamen and dissected to obtain different tissues, including gills, visceral mass, gonads, mantle, muscle and palps. There are six parallel samples for each tissue. The oyster larvae were obtained from the adult oysters. Sexually mature adults (three males and three females) were used in the collection of sperm and oocytes. After separately standing for 30 min, the sperm and oocytes were respectively mixed and incubated at different CO<sub>2</sub> concentrations (control 400 ppm, 1500 ppm, and 3000 ppm) at 25 °C for 10 min with gentle shaking. After insemination for 30 min, the unfertilized sperm were eliminated by washing with fresh filtered seawater. The oosperm were respectively distributed into a 60-L tank. After larval hatching, each tank was filled with different CO<sub>2</sub> concentrations of mixed gas to stabilize the pH. Two independent biological replicates of the control group and the experimental groups were prepared. The oyster larvae of the trochophore and D-veliger larvae (1, 2, and 4 days after post fertilization) were collected for quantitative RT-PCR, the WISH, and RNAi, respectively.

### 2.2. RNA preparation and cDNA synthesis

Approximately 50–100 mg of intact mantle, gill, adductor muscle, labial palp, visceral mass, and gonad tissues were collected by excision using sterile scissors. The samples were washed with 1 × 0.01 M phosphate buffered saline (PBS), directly frozen in liquid nitrogen, and stored at –80 °C, with three independent biological replicates for subsequent RNA extractions.

Each samples was thoroughly homogenized in TriZOL® using a Retsch MM400 tissue disruptor (Haan, Retsch, Germany), and incubated at room temperature for 5 min. Approximately 200 µL of chloroform

was added, vortexed for 15 s, and left to stand on ice for 5 min. The samples were then centrifuged at 12,000g for 15 min at 4 °C, and the supernatant was extracted. Equal volumes of isopropanol were added to the supernatant and incubated at 4 °C for at least 1 h. After incubation, the samples were centrifuged at 12,000g for 15 min at 4 °C, and the supernatant was discarded. Each RNA pellet was washed with 75% ethyl alcohol and vortexed, centrifuged at 12,000g for 5 min at 4 °C, the supernatant discarded, and the remaining ethyl alcohol was allowed to evaporate for about 10 min prior to adding 30 µL of DEPC water to re-suspend the pellet. RNA quantification was performed at wavelengths of 260 and 280 nm using a ND-2000 ultraviolet spectrophotometer (NanoDrop, U.S.) and RNA integrity was checked by 1.2% agarose gel electrophoresis.

Approximately 1 µg of extracted RNA was reverse transcribed using a PrimeScript RT reagent kit (TaKaRa, Dalian, China) according to the manufacturer's protocol. The cDNA mix was stored at –20 °C prior to cloning, whereas the remaining RNA was stored at –80 °C.

### 2.3. Cloning of *Ca-tyrA1*

The tyrosinase3-coding gene *Ca-tyrA1* was cloned using the 5'-full RACE and 3'-full RACE cDNA Amplification Kit (Takara) according to the manufacturer's instructions. Gene-specific primers (Table 1) were used in amplifying the *Ca-tyrA1* cDNA with polymerase Ex Taq (TaKaRa, Dalian, China) according to the following conditions: denaturation at 94 °C for 5 min, followed by 31 cycles at 94 °C for 30 s, 55 °C for 30 s, and 72 °C for 90 s. A final extension step was conducted at 72 °C for 10 min. Both purified PCR products were cloned into a pMD-19T vector and sequenced.

To confirm the accuracy of the sequence of *Ca-tyrA1* through the RACE, a pair of gene-specific primers, *Ca-tyrA1*-F1 and *Ca-tyrA1*-R1 (Table 1), were used for amplifying the *Ca-tyrA1* cDNAs with polymerase Ex Taq (Takara, China), according to the following conditions: denaturation at 94 °C for 5 min, followed by 31 cycles at 94 °C for 30 s, 56 °C for 30 s, and 72 °C for 90 s. As an extension, a final step was conducted at 72 °C for 10 min. The purified PCR products were cloned into a pMD-19T vector, transformed into competent DH5α cells, and sequenced in both directions as five independent clones.

### 2.4. *Ca-tyrA1* mRNA expression analysis in different larval developmental stages and subjected to acidification

The qRT-PCR primers were designed using Primer Premier 5.0, with cDNA sequences based on the full sequence of tyrosinase3-coding gene and primers synthesized by Invitrogen Trading Co., Ltd. (Shanghai, China). The sequence of the primers for qRT-PCR are listed in Table 1.

The first strand of the cDNA obtained from the extracted mRNA was used as template, and 2 µL were used for qRT-PCR using the ABI 7500 fast real-time PCR system (Applied Biosystems, Foster City, CA, US)

**Table 1**  
List of primers sequences used in this study.

Name	Experiment	Sequence(5'-3')
<i>Ca-tyrA1</i> -F	Confirm-PCR	AGATGCGGAAAGGACAACCTC
<i>Ca-tyrA1</i> -R	Confirm-PCR	CTCAGGCACACTCGACAA
<i>Ca-tyrA1</i> -F1	RACE	CAGGTCCAGCAGAAGAGCA
<i>Ca-tyrA1</i> -F2	RACE	AAGCCTTCCACATCCGATT
<i>Ca-tyrA1</i> -R1	RACE	TAAGCCCAAGCATCCTCAT
<i>Ca-tyrA1</i> -R2	RACE	CAAACAAGGAACGGGCTAC
UBQ-F	qRT-PCR	ATAGAGGCGTTGCATGAGC
UBQ-R	qRT-PCR	ACGGAGGACCAAGTGAAGG
EF-1α-F	qRT-PCR	ACCACCTGGTGAGATCAAG
EF-1α-R	qRT-PCR	ACGACGATCGCAITTTCTCT
<i>Ca-tyrA1</i> -F2	qRT-PCR	CAAGCAGGAACCTGGAGAGTC
<i>Ca-tyrA1</i> -R2	qRT-PCR	GGAGTGAAGCCAGGGCGAT
<i>Ca-tyrA1</i> -F3	WISH	CAAGCAGGAACCTGGAGAGTC
<i>Ca-tyrA1</i> -R3	WISH	GGAGTGAAGCCAGGGCGAT

with the SYBR green qPCR kit (ThermoFisher Scientific, US). PCR cycles were conducted using the following settings: denaturation at 95 °C for 10 min, followed by 40 cycles at 95 °C for 20 s, 55 °C for 20 s, and 72 °C for 20 s. All PCR experimentation was performed in triplicate, and standard curves were constructed for each reference cDNA sample. The purified PCR products were cloned into a pMD-19T vector and sequenced. The data represents the mean values of six biological replicates. Data of competitive real-time PCR analysis subjected to one-way analysis of variance (ANOVA) and followed by a multiple comparison test by using the LSD-*t*-test to determine the difference in mean values was used with the SPSS software. The P value for significance was set at  $P \leq 0.05$ .

### 2.5. WISH analysis

The digoxigenin-labeled cRNA probes were synthesized with a dig-RNA labeling kit (Roche). A fragment of the *Ca-tyrA1* cDNA was inserted into a pMD-19T EASY vector (Promega) and sequenced. The plasmid was used as template to amplify the *Ca-tyrA1* cDNA fragment, which was then utilized as the template for *in vitro* transcription. Riboprobes were synthesized by transcribing with T<sub>7</sub> RNA polymerase and digoxigenin-11-UTP (Roche). For WISH analysis, gastrulae, trochophores, early D-veliger larvae, three-day veliger larvae, and five-day D-veliger larvae were relaxed in 1 M MgCl<sub>2</sub> of filtered seawater (FSW) and then fixed in paraformaldehyde in PBS (4% PFA, pH 7.4) for 2 h. The fixation solution was then replaced, and then again fixed in fresh fixation solution at 4 °C overnight. The fixative was removed with three PBS washes, and then the samples were dehydrated in a methanol series gradient and stored at -20 °C until use. The WISH procedure used for spatial expression analysis was based on the protocol used in ascidians (Hinman and Degnan, 2000), with some modifications. The process of WISH was described in detail previously (Yang et al., 2012). Images were captured using a digital camera (Olympus DP71) that was attached to a fluorescence light microscope (Olympus BX51). Digital photographs were imported into Adobe Photoshop CS and cropped, and the brightness and contrast optimized.

### 2.6. Scanning electron microscopic observation

The trochophore larvae at about 11 h post fertilization were collected and fixed in 4% paraformaldehyde at 4 °C overnight. The larvae were then washed with PBS and re-fixed in fresh osmic acid for 1.5 h. After that the larvae were washed in PBS and then dehydrated in an ascending series of ethanol. At last, the larvae were stored in tertiary butanol at 4 °C overnight. A day after freeze drying, larvae were coated with gold and observed under a scanning electron microscope (SEM).

### 2.7. dsRNA synthesis

dsRNA synthesis was performed as described elsewhere (Fabioux et al., 2009). The region encompassing positions 1119 to 1373 of the *Ca-tyrA1* cDNA were amplified from the total extracted mRNA and the purified PCR products were subcloned into a pMD-19T vector (Takara) and sequenced.

For *in vitro* transcription, dsRNA was performed in 500- $\mu$ L PCR tubes. All instruments and reagents were RNase-free. The PCR reaction system consisted of the following components: 20  $\mu$ L of 5  $\times$  T7 transcription, 4  $\mu$ L of a 25 mM NTP mix, 2  $\mu$ g of linear template DNA, 4  $\mu$ L of T7 RNA polymerase, 3  $\mu$ L of a Ribolock RNase inhibitor, and RNase-free water to a final reaction volume of 100  $\mu$ L. The tubes were incubated at 37 °C for 4 h, and then 2  $\mu$ L of DNase was then added, followed by another incubation at 37 °C for 15 min to allow digestion of the DNA template. The reaction was terminated by adding 5  $\mu$ L of 0.5 M EDTA and incubating for 2 min at room temperature. RNA precipitation was performed by adding 10  $\mu$ L of 4 M LiCl, 300  $\mu$ L of pure ethyl alcohol, incubating at -80 °C for 4 h, centrifugation at 14,000 rpm for 15 min at 4 °C for

two cycles. The RNA pellet was suspended in 50  $\mu$ L of RNase-free water. Finally, 1  $\mu$ L of the RNase inhibitor was added to each of synthetic dsRNA to prevent possible degradation. Finally, the dsRNA was analyzed by 1% agarose gel electrophoresis and quality and quantity were assessed by using a ND-1000 ultraviolet spectrophotometer (NanoDrop, US).

### 2.8. *Ca-tyrA1* RNAi

RNAi was performed according to Huvet et al. (2012) and Fabioux et al. (2009). The oyster larvae were cultivated as described in Section 2.1. After the larvae reached the trochophore stage, these were soaked with the synthetic dsRNA at a final concentration is 100 ng/ $\mu$ L. The control group was soaked in seawater using the same volume. When the control group reached the early D-veliger stage, the larvae were anesthetized in MgCl<sub>2</sub> solution and fixed in 4% PFA. After 24 h, the solvent was replaced with fresh 4% PFA. Finally, images of the larvae were captured using a digital camera (Olympus DP71) that was attached to a microscope (Olympus BX51). The deformity rate of the larvae at the D-veliger stage was calculated based on the pictures of larvae after *Ca-tyrA1* RNAi.

## 3. Results

### 3.1. Sequence analysis

The *Ca-tyrA1* cDNA sequence and deduced amino acid sequence are shown in Fig. 1. The open reading frame was 1896 bp in length and encoded a protein of 631 amino acid residues. The full-length of the cDNA was 2430 bp, which included a 26-bp 5' untranslated region that was located at upstream of the putative start codon (ATG) and a 432-bp 3' untranslated region that ended with a poly(A) tail sequence. A putative polyadenylation signal (AATAAA) was located at position 2399, which is upstream of the poly(A) tail and separated by 16 nucleotides. The molecular weight of the protein was predicted to be 74.07 kDa, with a pI of 9.39. The deduced protein included a putative signal peptide of 24 amino acids, a transmembrane region (Fig. 1), and two putative major domains: Cu (A) site and Cu (B) site. Phylogenetic analysis indicated that *Ca-tyrA1* is a secreted protein belong to type A tyrosinase (Fig. 2), which was from the gene expansion of tyrosinase family.

### 3.2. Tissue distribution of *Ca-tyrA1*

To gain insights into the possible physiological functions of *Ca-tyrA1*, tissue-specific expressions of *Ca-tyrA1* were analyzed using quantitative RT-PCR. The expression pattern of *Ca-tyrA1* varied among tissues, and the highest *Ca-tyrA1* expression level was observed in the mantle and the lowest level in the visceral mass (Fig. 3). The expression level of *Ca-tyrA1* in the mantle is at least nine-fold higher than that in the other tissues.

### 3.3. *Ca-tyrA1* expression pattern during oyster larval development

The expression pattern of the *Ca-tyrA1* gene at different developmental stages after acidification was also measured by quantitative RT-PCR analysis. Fig. 4 shows that *Ca-tyrA1* mRNA was mainly expressed at the trochophore and early D-veliger stages and was particularly high in the trochophore. However, with larval development, the expression of *Ca-tyrA1* rapidly decreased and was almost zero in the 4-day-old D-veliger. After acidification treatment, a change in the level of mRNA expression of *Ca-tyrA1* was observed but was not statistically significant. However, the *Ca-tyrA1* mRNA levels in the 3000 ppm treatment group was significantly upregulated, whereas that in the 1500 ppm treatment group did not significantly differ ( $P > 0.05$ ) in the early D-veliger stage compared to that in the control group. The level

```

1      GGCCTCCGGACAATCAAGAAATCCAAGATGGCGAAAGGACAACCTCAACTTTATCGTCTGCTTCTTAGCAACGGTAGTCTTCCGGACATCTT
1      M R K G Q L N F I V C F L A T V V L P T S
91     TCGGATTAATGAAGAAATACAAACACCCCGTGATATCTCGAATGCTGTACTACAAATCTCAGAAGTCAACCATAGGCGAAGTTTCAG
22     F G L I E E I Q T P R D I L E C L I Y K S Q N S T I G E V S
181    GAAGAACGATCCAAGGTTTTCGCATCCGTAATTCACCCCTGGACACCCAGAGCGGCAAGAGAAGTTCGCGAAGAACATTTCTACTGAAAG
52     G R T I Q G F C I R K F T L D T Q S G K E N F A K N I S T E
271    GTGTGCAGTACCTTAAGTCCCTGTTTAGACAGCTAGAAATCAGAGGTTACGATCAGAAACGAGGAAAAAGACAAGCAGGAACTGGAGAG
82     G V Q Y L K S L F R Q L E S E V H D Q K R G K R Q A G T W R
361    TCCGAAGAGAGATCGGAACACTCAGCGATGCCGAGAGAAACAACGTTTCCAAATGCTTAAGAAGACTCAAGGGCGACTATTCTATTGATC
112    V R R E I G T L S D A E R N N V F Q C L R R L K G D Y S I D
451    CCAGAAATGAGTACATATGACCTGATCGCCCTCGCTTCACTCCGACAAGCTGCCCGCATGATGCACAATGAGCCCGCTTCTCCCGCCGCG
142    P R M S T Y D L I A S L H S G Q A A R M M H N G P A F L P P
541    ACATGGTTTATCTCCCTGGTAATGGAACTGCCGTGCGGGTACCCATGCCTTACTGGGACATGACTACTGACAGCGAGATGATGGACCCCA
172    H M V Y L L V M E T A C R V P M P Y W D M T T D S E M M D P
631    CCACCTCCATCGTTGGTCTGATCTTCTTTGGACCCGCAATGGACCAGTTCTGACTGGACCCCTTTGGAAGATTGAGAACCCCACTG
202    T T S I V W S D L F F G P G N G P V L T I G P F G R F R T P T
721    GAACCCCAATCATCAGAAACATTGGATCAGGTGGAGCTTCTCTGGCTAGAAAAGCTGGAATCAGAGCCTTCTGCTCCAGGAGAAAGGACAT
232    G T P I I R N I G S G A S L A R K A G I R A L L S R R T
811    TTGAGATCTCCGAGCCACAGCCAGCTCAAAGCATTITCTCTATCGAGGTTTCATCACAATGGCGTCCATAAATACATCGACGTTACATGT
262    F E I S E P Q P A Q S I F S I E V H H N G V H N Y I D G Y M
901    CTGGTCTTAACACAGCTTCTTGGGACCCAGTCTTCTGGTTCATCCACTTITCTTCCAACTCCTGTTGGGTTGCGTTCAGAAACGGTCAAA
292    S G L N T A S W D P V F W F I H S F F Q L L W V A F R N G Q
991    GAGCTAACCGCATCAACCCAGAGAGGATTACCCAAAGAGGAGTTCCAGTTCCAGCTGGTCATGAATTTTACCAAGAAATGAATTTTATGTC
322    R A N G I N P E R D Y P R G V R V P A G H E F Y Q R M N F M
1081   CATTCATGCGAAGAACACGAACTCGGAAGGATTATCCAACAGGATGACCCGATTTGTCAGTATGCTCCCATGCCAAGATGCCCGGCTT
352    P F M R R I T N S E G L S N R Y D R I V Q Y A P M P R C P A
1171   GTGGAGGTAGCCCGTTCCTTGTGTTGCTCCGAGGCGTATGCGTGTCCAGGTCAGCAGAGAGCACCTGTTTTCTTCAGAGGAAAGCAA
382    C G G S P F L V C L R G V C V S R S S R R A P V F R G K R
1261   GCGTGGCACTTCAGGGATCAGTTGGCCGATGAAAACGTTAACCCCAACCCACTAATTTAATCAATCAATGAAGCAGCTCTCTCAA
412    S A G T S G D Q L A D E N V N P N T T M L I Q S N E A A L S
1351   CGCTAAATAAGCCCTACCAGAATACCTTTATGATCGACGGAAGAAATGATGAGGATGCTTGGGCTTACATTCCTATTAGGGTCTTATACG
442    T L N K P Y Q N T F M I D G K I D E D A W A Y I P I R V L Y
1441   AAAGACCAAAAGGCTTAACTTTCATACCATCACCAGGAGCTACAAAAGAGATATGTACGATCTGAAAACCTTAAAGAAATGAAGCAA
472    E R P K G F N F H T T S P G A T K R D M Y D P E N F K N E A
1531   AGAAGATAGGACTTCAATGAAGTACAGTACAAGCAACAGTGCATCCGCTGGATCCGGAGCAGCAAGGTTTTGTGTCAGTCTAATG
502    K R I G L H N E V Q Y K Q C T P S G S G A A K V F V Q N G
1621   GACTCAATTACGCAGGCAAAATACAAAGATTATGCAATCGTCGATGAAAGGCAACCAGTAAATCAGCAATTAATGATGAGGATTAAGA
532    G L N Y A G K Y K D Y A I V D E R Q P V T S A I T Y V G F K
1711   AGCCTTCCACATCCGATTCAGAGGTTATTTTAAACAGCTTACGATACCTGTGGGCGCATCTGTCCGACCGCTTGTCCAGTGTATGGTCATC
562    K P S T S D S E V I L T A Y D T C G R I C R P A C P V Y G H
1801   ATCGGAAATCTATAGAGCGTGCACAGTAGCTTCCGAAATTTCCCAATCACTTATGTTTAGTCAAAAATACGGGAAGCGCGGT
592    H R E S Y R A C S G S F R I S S K S P L M F S Q N Y G S A V
1891   CCTCTACATGGAATGTTAGGGAGATGGAACAGGATGTAAGAGTAGTCAATCCCTACCGATCATTGTTATGTGACCCCAAAAATTCCT
622    S S T W N V R E M E P G C K S S Q S L P I T F V C D H Q N S
1981   GGCCATGGGAATCAAACTGTAATAAATTAAGGGTAACATCTTCAAAGTATTAACCAAAAACCTCAGAGAGAATCAATCCATGAGAT
652    W P W E S K L *
2071   AGTTTTCTTCAATTAAGCAAAGTTGTATAACTTTAATTAACAGTTTGTCTCATCTTAAACTACATCAAGCAGTAAACGAAATATG
2161   TACCTTATTCAGTCGTTGAAATGAACAGATAATTTTTTCATTGTAATCAAAAGGTTAATTTACCTAAACGATTAATTTTAGTTG
2251   TTAATACCGCTACTCATAATGAGTGTCTTTTCTCCCTCCATTGTTGTCGATGTGCAAGTCTTTCAGTTTGTATAATTTATTTGTC
2341   GAGTGAGTGCTGAGACTGAATGTACTGTGGCAGTGAATAGTGAATGCTTTGTAATATAATCAAAAATCCATATGAGAATGTTAAAA
2431   AAAAAA
    
```

**Fig. 1.** *Ca-tyrA1* full-length cDNA and deduced amino acid sequence from *C. angulata*. The promoter sequence (ATG) and translation termination codon (TAA) are boxed in green and red. The signal peptide is underlined in blue and the stop codon is indicated by \*\*\*. The transmembrane region is underlined in red. The N-myristoylation site is respectively indicated in yellow boxes. Two copper-binding domains (CuA and CuB) were implied in black and blue boxes. The single polyadenylation signal sequence and the ployA sequence are indicated by thick black bars.

of *Ca-tyrA1* mRNA expression increased and then rapidly decreased in the treatment groups and the control group ( $P > 0.05$ ) as the larvae progressed from the early D-veliger to the terminal D-veliger stages. Data analysis revealed that *Ca-tyrA1* transcription mainly occurred at the trochophore stage in all groups, when the periostracum could be initially observed (Mouëza et al., 2006).

**3.4. Spatial-temporal expression of *Ca-tyrA1* mRNA in different larval developmental stages**

By WISH, we detected the expression of *Ca-tyrA1* mRNA in the different stages of larval development. Fig. 5 shows that the expression of *Ca-tyrA1* mRNA first occurs at the gastrula stage and persists until the early D-veliger stage. With larval development, *Ca-tyrA1* mRNA was expressed at the edge of gastrula, and when the larvae developed

to the early D-veliger stage, the signal shape was similar to the initial non-calcified shell (IaCaS).

**3.5. SEM observation of the *C. angulata***

Through scanning electron microscopy (SEM) combined with energy disperse spectroscopy analysis, we observed the formation of the IaCaS. The IaCaS appears in the shape of a saddle during the early D-veliger stage (Fig. 6).

**3.6. RNAi**

To determine the role of *Ca-tyrA1* in InCaS formation in *C. angulata*, an RNAi experiment using larvae from the gastrula to the early D-veliger stages was performed. Fig. 7a shows that the deformity rate of the group

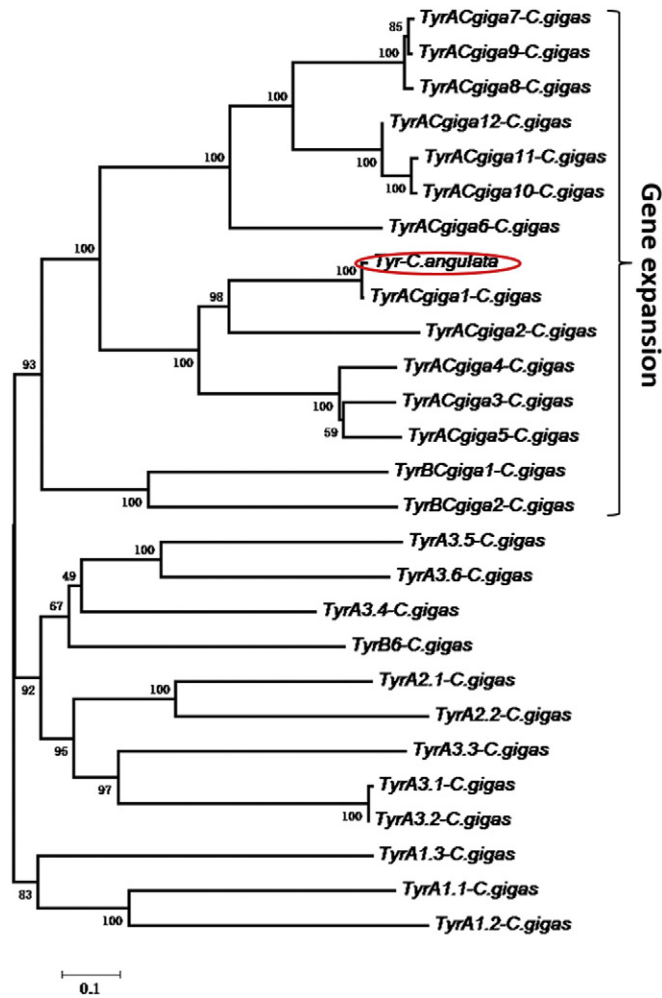


**Fig. 2.** Phylogenetic tree analysis of *Ca-tyrA1* from *C. angulata* with other tyrosinases from *C. gigas* using MEGA 5. The amino acid sequence alignment was carried out by Clustal × 1.8 program, and the dendrogram was constructed by the neighbor-joining method of clustering based on a PAM Matrix. Bootstrap values were computed over 1000 replications.

after the RNA interference was significantly higher (66.7%) than that in the control group (2.7%). Microscopy analysis also revealed that the edge of the shell from the abnormal larvae was incomplete or broken (Fig. 7B).

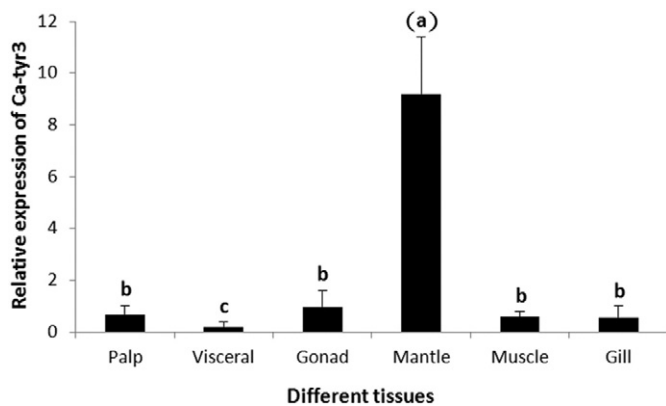


**Fig. 3.** Expression analysis of *Ca-tyrA1* mRNA transcripts in different tissues of adult variously oyster analyzed using quantitative real-time PCR. Each bar represents the mean ± SD of three replicates. Data with significant difference between each other at  $P < 0.05$  are indicated by different letters above the bars.

#### 4. Discussion

The tyrosinase gene family has been reported to be classified into three types: secreted form (Type A), cytosolic form (Type B) and membrane-bound form (Type C) based on the arrangement of histidine, (Aguilera et al., 2014). In the Pacific oyster all the tyrosinases belong to Type A just by the arrangement of histidine, but in the Pacific oyster some tyrosinase including signal peptide belong to secreted form (Type A) and other tyrosinase locate in the plasma membrane (Type B) or has the transmembrane domain in the protein sequence (Type B), especially some tyrosinase both include the signal peptide and the transmembrane domain (Yu et al., 2014a). In the present study, we cloned and characterized another tyrosinase gene from *C. angulata*, which we have designated as *Ca-tyrA1*. *Ca-tyrA1* is a member of the type 3 copper protein superfamily, which includes arthropod phenoloxidas and hemocyanins. It contains a putative signal peptide, suggesting that it is a secreted protein, and has a transmembrane domain which overlap with the signal peptide (Yu et al., 2014a). *Ca-tyrA1* has two copper-binding domains, namely, the Cu(A) site and Cu(B) site, which are the main features of the tyrosinase superfamily and tyrosinase gene from *C. gigas* (Huan et al., 2013). The two copper-binding domains consist of an oxygen-binding active center (Cuff et al., 1998; Morrison et al., 1994; Decker and Tuzcek, 2000). Comparison of the two sites in the tyrosinase protein from other organisms show that the six histidine residues are copper-binding ligands, which is arranged in similar positions in the molluscan tyrosinase (Alvaro et al., 1995). Furthermore, several amino acid residues around the six copper ligands are also conserved in molluscs (Zhang et al., 2006). The oyster of *C. gigas* has multiple tyrosinase genes which has undergone independent lineage-specific gene expansions (Zhang et al., 2012; Aguilera et al., 2014; Yu et al., 2004b), the expansion gene were indicated in the phylogenetic tree, the phylogenetic tree analysis imply that the tyrosinase gene obtained from *C. angulata* belong to secreted form (Type A1) in the expansive genes.

Previous studies have focused on the roles of tyrosinases in adult shells (Nagai et al., 2007). Expression pattern analysis has indicated that *Ca-tyrA1* is differentially expressed in various tissues, and the highest level of expression occurs in the mantle, consistent with that of *CgTyr2* in *C. gigas* (Yu et al., 2014a). This finding suggests that the tyrosinase gene is involved in periostracum formation in adult bivalves, and that *Ca-tyrA1* is involved in the adult shell formation in *C. angulata*. Our qRT-PCR analysis of different larval developmental stages showed that *Ca-tyrA1* was highly expressed in the trochophore stage, which represents the time of InCaS formation, thereby suggesting that *Ca-tyrA1* may be involved in InCaS formation. Ocean acidification largely impacts the calcification of marine invertebrates, which is the process of generating calcium carbonate (Zhao and Liu, 2015). Furthermore, several studies have shown that ocean acidification strongly affects the expression of shell formation-related genes (Haruko et al., 2012; Evans and Watson-Wynn, 2014; Paulina et al., 2012). We also evaluated the expression pattern of *Ca-tyrA1* in different larval developmental stages under acidification conditions. As shown in Fig. 4, *Ca-tyrA1* was highly expressed in larval trochophore stage in both control group and acidification conditions, but on the 3000 ppm acidification conditions, the *Ca-tyrA1* expression level was still high in one day of D-type stage, meanwhile the level in control and 3000 ppm were down-regulation, these observations indicated that oyster larvae can endure acidification within limits by regulating gene expression pattern (Gehler et al., 2016). Moreover these results imply that *Ca-tyrA1* is significantly upregulated in the D-veliger larva, thereby compensating for the damages in shell formation that were incurred during ocean acidification.

To determine the function of *Ca-tyrA1* in relation to InCaS formation in different larval stages of development, we conducted WISH analysis. The development of fertilized oocytes of *C. angulata* is consistent with the normal pattern in mollusks (Moužea et al., 2006). As shown in Fig. 5, *Ca-tyrA1* expression occurs in gastrula stage in localized area,

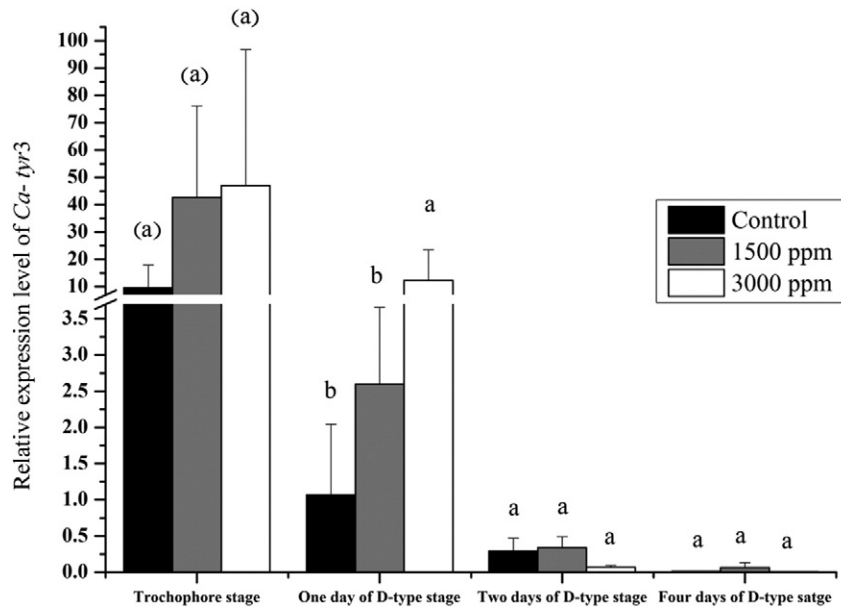


**Fig. 4.** *Ca-tyrA1* expression in different development stages of larval *C. angulata* after exposed to ocean acidification. Each bar represents the mean  $\pm$  SD of three replicates. Data with significant difference between each other at  $P < 0.05$  are indicated by different letters above the bars.

when larvae develop into the trochophore stage the signal region became larger, which indicated that *Ca-tyrA1* expression level was higher than that in gastrula stage, moreover the result in Fig. 4 showed that *Ca-tyrA1* expression was high in the trochophore stage comparing in D-type larval stage in the control group. The InCaS was first formed during the trochophore stage, and our results indicated that *Ca-tyrA1* was mainly expressed in the trochophore, particularly at the edge of the InCaS, as compared to that observed during SEM analysis. These observations were consistent with the results of tyrosinase 1 from *C. gigas*

(Huan et al., 2013). Previous studies on genes involved in shell formation mainly focused on the regulatory or biomineralization genes (Nederbragt et al., 2002; Liu et al., 2007; Fang et al., 2011; Gardner et al., 2011), whereas the present study shows that *Ca-tyrA1* plays an important role in the formation of the periostracum of the larval shell.

Classic functional genetic approaches such as mutagenesis are not yet available for application to bivalve molluscs (Elbashir et al., 2001). RNAi is an alternative method for reverse genetics, which is a fast and effective technique for detecting the loss-of-function phenotype of a

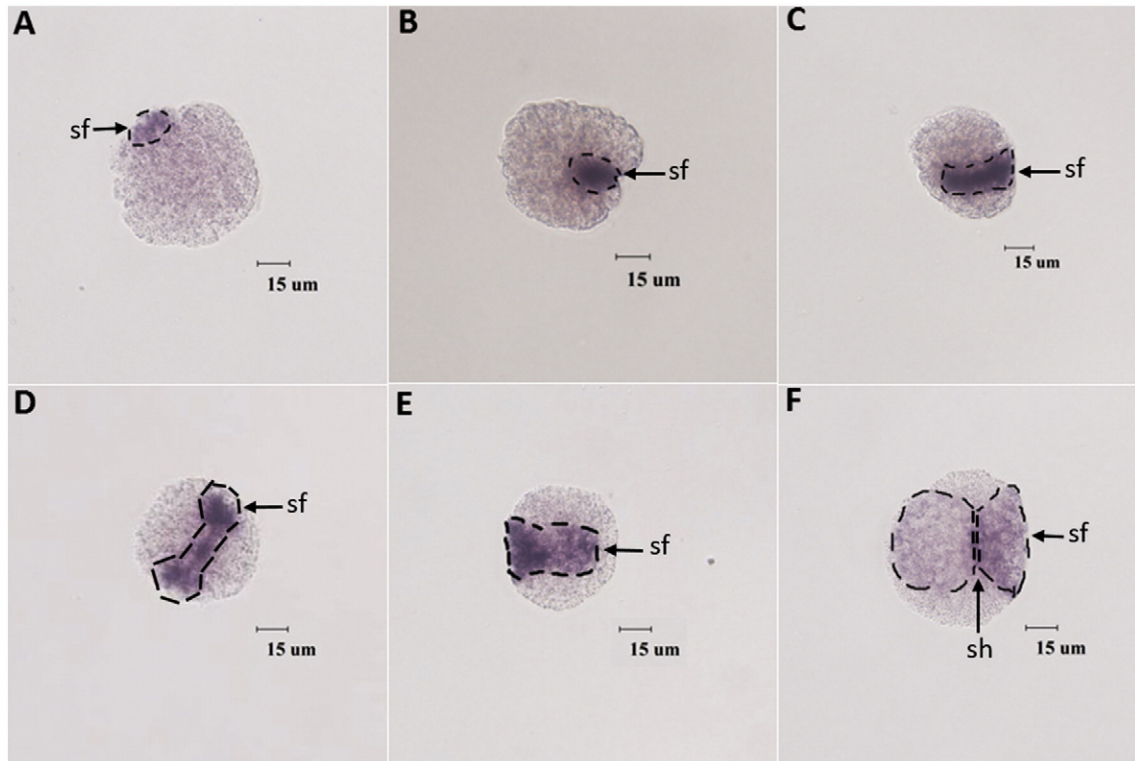


**Fig. 5.** Distribution of *Ca-tyrA1* during development from gastrula to early D-veliger by whole mount *in situ* hybridization. A: gastrula; B, C, D and E: trochophore; F: D-veliger. The scale of black bar is 15  $\mu$ m. The black dotted lines indicated the saddle-like shell field (sf, arrows), and the shell hinges (sh, arrows) were indicated by double lines.

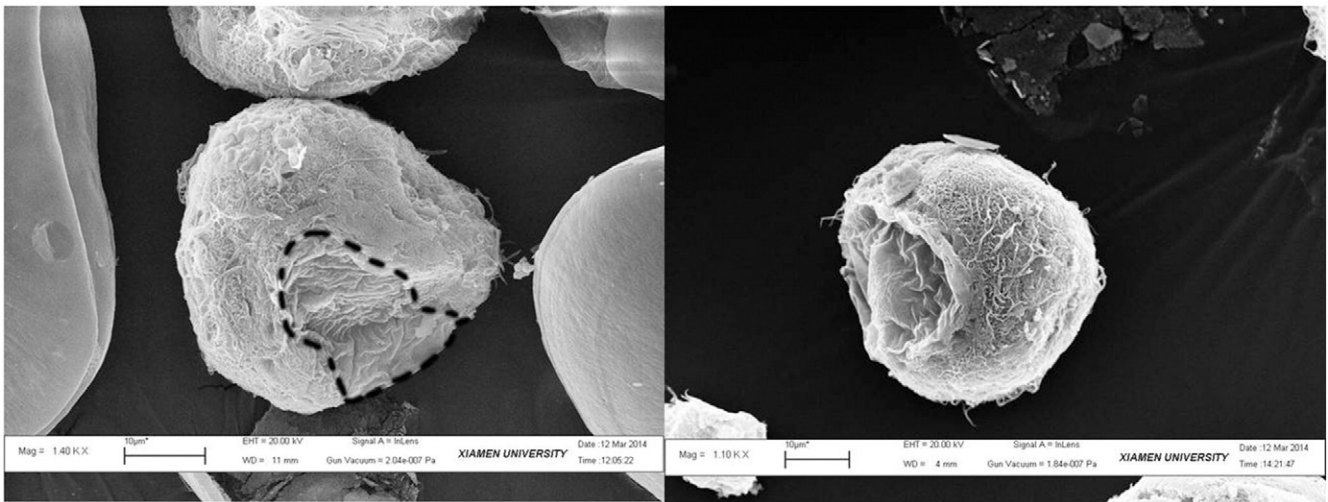


Fig. 6. SEM observation of larvae in trochophore from the oyster *C. angulata*. Black dotted lines indicated the saddle-like shell field.

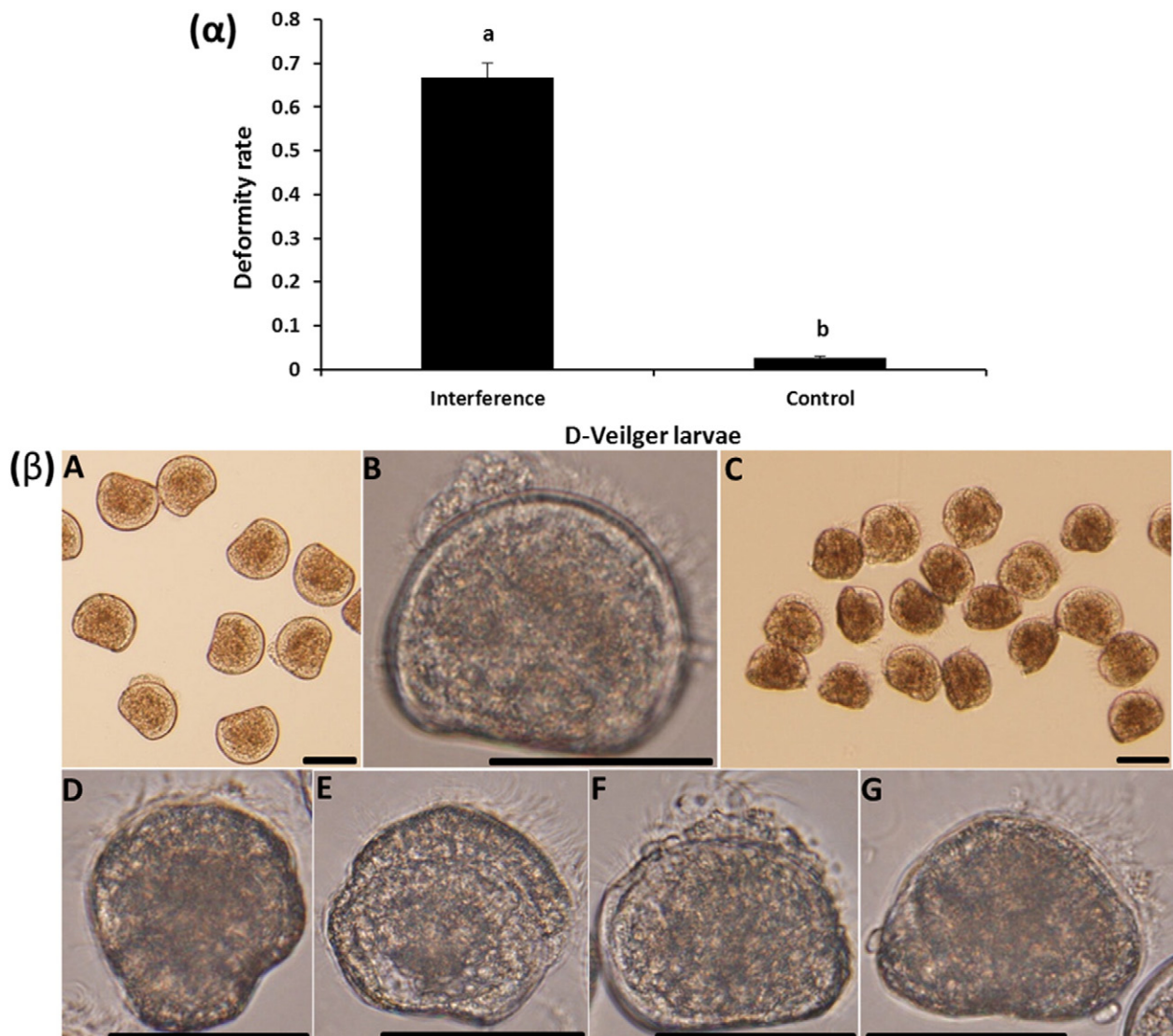


Fig. 7. Calculation analysis of larval deformity rate ( $\alpha$ ) and the morphological observation of larval ( $\beta$ ) after *Ca-tyrA1* RNA interference. Data with significant difference between each other at  $P < 0.05$  are indicated by different letters above the bars. A and B: the control group; C, D, E, F and G: the larval group after *Ca-tyrA1* RNA interference. The scale of black bar is 50  $\mu\text{m}$ .

gene (Fire et al., 1998). Long dsRNAs have been shown to undergo efficient gene silencing in invertebrates (Elbashir et al., 2001). The expression of *tyr3* appears to be restricted to the domain of shell forming, and thus, RNAi was performed to detect the effect of *Ca-tyrA1* in InCaS formation. RNAi analysis showed that the *Ca-tyrA1* expression pattern of the larvae was disrupted after exposed with acidified conditions. Most of the abnormal larvae showed abnormal shapes or the edge of the shell was apparently broken, which was consistent with the result of WISH, which showed that the protein was mainly expressed at the edge of larvae. Tyrosinases are a big family of enzymes with phenol oxidase activity, and when larval development reached the trochophore stage, the expression of *Ca-tyrA1* was activated in the cells of the shell area, which in turn catalyzed the formation of the InCaS. However, when the trochophore stage the *Ca-tyrA1* expression was disturbed and then the function of *Ca-tyrA1* in the high expression area was disrupted, the edge of the larvae after RNAi did not follow a normal pattern of formation. Based on these observations, we speculated that enzymes such as tyrosinase play a key role in larval shell formation. This phenomenon has also been observed in insects, and different enzymes play various roles in the hardening of the insect cuticle at various stages (Andersen, 2010).

In conclusion, we characterized a full-length cDNA that encoded a member of the type 3 tyrosinase family named as *Ca-tyrA1* from the oyster *C. angulata*. Through qRT-PCR and WISH expression pattern analyses indicated that *Ca-tyrA1* is upregulated in the mantle, thereby suggesting that *Ca-tyrA1* is involved in adult shell formation. In addition, at different larval developmental stages, *Ca-tyrA1* is mainly expressed in the area of the InCaS in the trochophore, thereby indicating that the function of *Ca-tyrA1* is probably related to larval shell formation. To confirm the role of *Ca-tyrA1*, RNAi was performed, which further proved that *Ca-tyrA1* plays an important function in larval shell formation.

### Conflict of interest

All the authors in this manuscript have no conflict of interest.

### Acknowledgements

This study was funded by NSFC (No. 41176113), Marine nonprofit industry research special funds (No. 201305016), the Earmarked Fund for Modern Agro-industry Technology Research System (No. nycytx-47), the National Natural Science Foundation of China under Grant (41276127), the Regional Demonstration Projects for Innovation and Development of Marine Economy in Xiamen under Grant (12PZB001SF09), Young and middle-aged teachers education scientific research project of Fujian (No. JA15811) and Science and technology research program of Xiamen city (No. 3502Z20154078).

### References

- Aguilera, F., McDougall, C., Degnan, B.M., 2014. Evolution of the tyrosinase gene family in bivalve molluscs: independent expansion of the mantle gene repertoire. *Acta Biomater.* 10, 3855–3865.
- Alvaro, S.F., Rodríguez-López, J.N., Canovas, G., García-Carmona, F., 1995. Tyrosinase: a comprehensive review of its mechanism. *Biochim. Biophys. Acta* 1247 (1), 1–11.
- Andersen, S.O., 2010. Insect cuticular sclerotization: a review. *Insect Biochem. Mol. Biol.* 40 (3), 166–178.
- Chang, T.S., 2009. An updated review of tyrosinase inhibitors. *Int. J. Mol. Sci.* 10 (6), 2440–2475 (2009).
- Checa, A., 2000. A new model for periostracum and shell formation in Unionidae (*Bivalvia*, *Mollusca*). *Tissue Cell* 32 (5), 405–416.
- Cuff, M.E., Miller, K.I., van Holde, K.E., Hendrickson, W.A., 1998. Crystal structure of a functional unit from octopus hemocyanins. *J. Mol. Biol.* 278, 855–870.
- Decker, H., Tuczek, H., 2000. Tyrosinase/catecholoxidase activity of hemocyanins: structural basis and molecular mechanism. *Trends Biochem. Sci.* 25, 392–397.
- Elbashir, S.M., Harborth, J., Lendeckel, W., Yalcin, A., Weber, K., Tuschl, T., 2001. Duplexes of 21-nucleotide RNAs mediate RNA interference in cultured mammalian cells. *Nature* 411, 494–498.

- Evans, T.G., Watson-Wynn, P., 2014. Effects of seawater acidification on gene expression: resolving broader-scale trends in sea urchins. *Biol. Bull.* 226 (3), 237.
- Fabioux, C., Corporeau, C., Quillien, V., Favrel, P., Huvet, A., 2009. In vivo RNA interference in oyster-*vasa* silencing inhibits germ cell development. *FEBS J.* 276 (9), 2566–2573.
- Fabry, V.J., Seibel, B.A., Feely, R.A., Orr, J.C., 2008. Impacts of ocean acidification on marine fauna and ecosystem processes. *ICES J. Mar. Sci.* 65 (3), 414–432.
- Fang, D., Xu, G., Hu, Y., Pan, C., Xie, L., Zhang, R., 2011. Identification of genes directly involved in shell formation and their functions in pearl oyster *Pinctada fucata*. *PLoS One* 6 (7), e21860.
- Fire, A., Xu, S., Montgomery, M.K., Kostas, S.A., Driver, S.E., Mello, C.C., 1998. Potent and specific genetic interference by double-stranded RNA in *Caenorhabditis elegans*. *Nature* 391, 806–811.
- Gardner, L.D., Mills, D., Wiegand, A., Leavesley, D., Elizur, A., 2011. Spatial analysis of biomineralization associated gene expression from the mantle organ of the pearl oyster *Pinctada maxima*. *BMC Genomics* 12, 455.
- Gehler, A., Gingerich, P.D., Pack, A., 2016. Temperature and atmospheric CO<sub>2</sub> concentration estimates through the PETM using triple oxygen isotope analysis of mammalian bioapatite. *PNAS* 113 (28), 7739–7744.
- Haruko, K., Yoshiki, T., Daisuke, K., Koji, A., 2012. Ocean acidification reduces biomineralization-related gene expression in the sea urchin, *Hemicentrotus pulcherrimus*. *Mar. Biol.* 159 (12), 2819–2826.
- Hinman, V.F., Degnan, B.M., 2000. Retinoic acid perturbs *Otx* gene expression in the ascidian pharynx. *Dev. Genes Evol.* 210, 129–139.
- Hofmann, G.E., Barry, J.P., Edmunds, P.J., Gates, R.D., Hutchins, D.A., Klinger, T., Sewell, M.A., 2010. The effect of ocean acidification on calcifying organisms in marine ecosystems: an organism-to-ecosystem perspective. *Annu. Rev. Ecol. Syst.* 41, 127–147.
- Huan, P., Liu, G., Wang, H.X., Liu, B.Z., 2013. Identification of a tyrosinase gene potentially involved in early larval shell biogenesis of the Pacific oyster *Crassostrea gigas*. *Springer-Verlag Berlin Heidelberg. Dev. Genes Evol.* 2013, 389–394.
- Huvet, A., Fleury, E., Corporeau, C., Quillien, V., Daniel, J.Y., Riviere, G., Boudry, P., Fabioux, C., 2012. In vivo RNA interference of a gonad-specific transforming growth factor-beta in the Pacific oyster *Crassostrea gigas*. *Mar. Biotechnol.* 14 (4), 402–410.
- Li, J.Q., Jiang, Z.J., Zhang, J.H., et al., 2013. Detrimental effects of reduced seawater pH on the early development of the Pacific abalone. *Mar. Pollut. Bull.* 74 (1), 320–324.
- Liu, H.L., Liu, S.F., Ge, Y.J., Liu, J., Wang, X.Y., Xie, L.P., Zhang, R.Q., Wang, Z., 2007. Identification and characterization of a biomineralization related gene PFMG1 highly expressed in the mantle of *Pinctada fucata*. *Biochemistry* 46, 844–851.
- Marin, F., Luquet, G., 2004. Molluscan shell proteins. *C. R. Palevol* 3 (6), 469–492.
- Morrison, R., Mason, K., Frost-Mason, S., 1994. A cladistic analysis of the evolutionary relationships of the members of the tyrosinase gene family using sequence data. *Pigment Cell Res.* 7, 388–393.
- Mouëza, M., Gros, O., Frenkiel, L., 2006. Embryonic development and shell differentiation in *Chione cancellata* (Bivalvia, Veneridae): an ultrastructural analysis. *Invertebr. Biol.* 125 (1), 21–33.
- Nagai, K., Yano, M., Morimoto, K., Miyamoto, H., 2007. Tyrosinase localization in mollusk shells. *Comp. Biochem. Physiol. B* 146 (2), 207–214.
- Nederbragt, A.J., van Loon, A.E., Dictus, W., 2002. Expression of *Patella vulgata* orthologs of *engrailed* and *dpp-BMP2/4* in adjacent domains during molluscan shell development suggests a conserved compartment boundary mechanism. *Dev Biol* 246, 341–355.
- Orr, J.C., Fabry, V.J., Aumont, O., et al., 2005. Anthropogenic ocean acidification over the twenty-first century and its impact on calcifying organisms. *Nature* 437, 681–686.
- Paulina, K., Paul, R.C., David, I.K., Rodriguez-Lanetty, M., David, J.M., Sophie, D., Ove, H.G., 2012. Major cellular and physiological impacts of ocean acidification on a reef building coral. *PLoS One* 7 (4), e34659.
- Shirayama, Y., Thornton, H., 2005. Effect of increased atmospheric CO<sub>2</sub> on shallow water marine benthos. *J. Geophys. Res. Oceans* (1978–2012) 110 (C9), C09S08.
- Talmage, S.C., Gobler, C.J., 2010. Effects of past, present, and future ocean carbon dioxide concentrations on the growth and survival of larval shellfish. *PNAS* 107 (40), 17246–17251.
- Valerio, M., Andrea, C., Marco, M., Livio, F., Monica, B., Maria, G.M., 2012. First evidence of immunomodulation in bivalves under seawater acidification and increased temperature. *PLoS One* 7 (3), e33820.
- Watson, S.A., Peck, L.S., Tyler, P.A., et al., 2012. Marine invertebrate skeleton size varies with latitude, temperature and carbonate saturation: implications for global change and ocean acidification. *Glob. Change Biol.* 18 (10), 3026–3038.
- Wood, H.L., Spicer, J.I., Widdicombe, S., 2008. Ocean acidification may increase calcification rates, but at a cost. *Proc. Biol. Sci.* 275 (1644), 1767–1773.
- Yang, B.Y., Qin, J., Shi, B., Han, G.D., Chen, J., Huang, H.Q., Ke, C.H., 2012. Molecular characterization and functional analysis of adrenergic like receptor during larval metamorphosis in *Crassostrea angulata*. *Aquaculture* 366–367, 54–61.
- Yu, X., Yu, H., Kong, L.L., Guo, F.F., Zhu, G., Li, Q., 2014a. Molecular cloning and differential expression in tissues of a tyrosinase gene in the Pacific oyster *Crassostrea gigas*. *Mol. Biol. Rep.* 41, 5403–5411.
- Yu, X., Yu, H., Kong, L.F., Li, Q., 2014b. Phylogenetic analysis of tyrosinase gene family in the Pacific oyster (*Crassostrea gigas* Thunberg). *Hereditas* 36 (2), 135–144.
- Zhang, C., Xie, L., Huang, J., et al., 2006. A novel putative tyrosinase involved in periostracum formation from the pearl oyster (*Pinctada fucata*). *Biochem. Biophys. Res. Commun.* 342 (2), 632–639.
- Zhang, G.F., Fang, X.D., Guo, X.X., et al., 2012. The oyster genome reveals stress adaptation and complexity of shell formation. *Nature* 490 (7418), 49–54.
- Zhao, X.G., Liu, G.G., 2015. Advances in the effects of ocean acidification on marine invertebrates. *Acta Ecol. Sin.* 35 (7), 2388–2398.